



Fatigue Fracture Surface Analysis on Aluminium Reinforced Metal Matrix Composites on Chill Casting

Sunil Kumar M.^{1*}, Sathisha N.², Jagannatha N.³ and Batluri Tilak Chandra⁴

¹VTU-RRC, Belgam - 590018, Karnataka, India; sunilkumar@btibangalore.org

²Mechanical Engineering, YIT, Mangalore - 574225, Karnataka, India

³Mechanical Engineering, SJMIT, Chitradurga - 577502, Karnataka, India

⁴Mechanical Engineering, SSIT, Tumkur - 572 105, Karnataka, India

Abstract

In this manuscript, an effort has been made through study the influence of copper chill in Aluminium Metal Matrix Composites (AMMCs), and also to explore the fatigue behaviour of the prepared aluminium A356-Hematite particulate metal matrix composite, which is cast through sand casting practice without and with copper chills at ends to get isotropic and homogeneous substantial properties under liquid metallurgical manner by varying weight fraction particulates of Hematite ranges from 0wt% - 12wt% in phases about 3wt%. The test samples stood prepared as per ASTM standards. Experiments were conducted to study the fatigue behaviour using ducom-type fatigue testing equipment. The result reveals that the composites cast with copper chills show superior fatigue strength as compared to the composites cast without copper chills. The micrographic analysis is performed using XRD (X-Ray Diffraction) patterns and SEM (Scanning Electron Microscope) photos. The existence of Hematite particles was confirmed from XRD and also found that the uniform dispersal of Hematite particles in the A356 matrix alloy of composites cast with copper chills. It was also observed that the fine-grained structure is obtained due to rapid cooling which influences improved fatigue strength in the composites with copper chills. The fractured surface of crack initiation and propagation along with fractography was studied with aim of SEM photos. The fractography images show the mode of fracture which is brittle in nature, signified by the cleavage facets from the transgranular crystallographic plane and striations. It is also observed that an improved content of reinforcement in both without and with copper chill mixtures results in a substantial development in fatigue strength. Copper chill fatigue specimen show higher fatigue strength than without copper chill specimen.

Keywords: Al A356, Fatigue Strength, Fractography, Hematite, Microstructure

1.0 Introduction

Aluminum alloys are the most commonly used alloys in today's industries for better results. Due to their high toughness, hardness and strength, with better corrosion

and wear resistance, aluminum metal matrix composites are widely used in various areas such as automotive, military, and aviation¹⁻³. By adding hard iron ore particles known as Hematite into an aluminum matrix, its wear resistance properties were improved for applications in

*Author for correspondence

the field of wear and tear⁴. Sand casting with superior properties must be found by using metallic elements as end chills like copper, which have effects on the mechanical, microstructure and tribological properties^{4,5}. One of the most profitable and extensively used methods for MMCs castability is chilled casting through sand moulds using the liquid metallurgy process⁶. According to the other study, Vasanth Kumar, *et al.*,⁷ investigated the fatigue and fracture behaviour of casted Al6061 alloy with B₄C-reinforced composite. Results show that fatigue strength and fracture toughness of the mixtures were improved with the addition of the B₄C particles in wt.% of the strengthening. Mahendra HM, *et al.*,⁸ reported fatigue and fracture behaviour of an Al6061 alloy blend with different weight percentage of Al₂O₃ Metal Matrix Composite. The result shows that composites with a configuration of 4% Al₂O₃ improve the fatigue and fracture properties. The fatigue property and fracture stress are significantly impacted by Al₂O₃. Krishnaraj S, *et al.*,⁹ reported the fatigue behaviour of Al 6061 reinforced with different weight percentage of SiC, TiO₂, and magnesium (Mg) hybrid reinforced composite. At room temperature, a low-cycle fatigue study has been conducted on developed composites. The result shows that by adding reinforced particles to the hybrid composites, the strength has been increased. The hybrid composite shows higher fatigue strength than an as-cast alloy. Sanju, *et al.*,¹⁰ examine the fatigue and corrosion behaviour of Al LM13 strengthened with Hematite Metal Matrix Composite (MMCs). The results show that heat-treated fatigue specimens show higher fatigue strength than as-cast specimens and heat-treated corrosion test specimens show a lower corrosion rate than as-cast specimens. Achutha MV *et al.*,¹¹ reported the fatigue and mechanical properties of LM 25 aluminium alloy reinforced with hybrid composite for different weight percentage of silicon carbide and graphite particles were examined result shows, the fatigue life of hybrid Al-SiC-Gr composites containing 2.5 wt% is experimentally determined at different stress levels and associated with that of LM 25 alloy. While compared to the base alloy, LM 25, the hybrid composite displayed improved fatigue resistance. Myriounis DP, *et al.*,¹² reported fatigue behaviour of silicon carbide (SiC)-reinforced with A359 aluminium alloy matrix composite. A variety of heat treatments have been accomplished for the 20 vol. % SiCp composite. The results show that heat treated fatigue specimen shows higher fatigue strength than compared to unheat treated fatigue specimens. The heat treatment

had a significant impact on fatigue strength. S Ramesh, *et al.*,¹³ stated that the aluminium 6061 alloy is blended with diverse weight fractions of silicon carbide (SiC) and zirconium di-oxide (ZrO₂) manufactured by the stir casting technique. The composite having combinations of I. Al:SiC::100:5 and II. Al:ZrO₂:SiC::100:3:2 is used for experimentation. The result shows that as compared to composition I, IInd composition provides a higher value of hardness 53.6 RHN. A tensile strength of 96.43 N/mm² can be observed in composition II, as compared to 67.229 N/mm² in composition I. For composition II, the fatigue test indicates a life cycle to failure of 105 cycles, while it indicates a life cycle to failure of over 104 cycles for composition I, for stress varieties of 79.062 MPa and 150.651 MPa, respectively. Girija Moona, *et al.*,¹⁴ studied the fatigue properties of hybrid composites were prepared by reinforcing aluminium alloy with particulate reinforcements. The Al 7075-T6 alloy is reinforced with different weight fractions of eggshell, aluminium oxide and silicon carbide particles that were fabricated through an electromagnetic stir casting technique. The developed specimens are tested by means of a rotating beam fatigue testing machine. The Taguchi approach was conducted in order to produce hybrid AMMCs with improved fatigue resistance as per the L9 orthogonal array. An analysis of variance (ANOVA) was also used to detect the effect of diverse process constraints on the fatigue life of an established composite. The results show that hybrid composite samplings showed substantial enrichment in fatigue resistance in terms of revocable load cycles survived compared to as cast composite specimens. CS Ramesh, *et al.*,¹⁵ the researcher studied the fatigue behaviour of Al6061 alloy armored with Ni-P coated Si₃N₄ particles at different weight fractions fabricated through stir casting method. The developed composite subjected to hot forged at a temperature of 500°C using a 300T hydraulic hammer, Microstructural studies and fatigue strength test. Results reveal that the reinforcement content increased in both as-cast and hot-forged composites, showing substantial enhancement in fatigue strength. The fatigue strength of hot forged alloys and composites is higher than that of cast matrix alloys.

A past study of the literature found that there has been less/little work done on fatigue behaviour studies on A356-Hematite particulate composites.

An effort has been made in this study to investigate fatigue fracture behaviour on the effect of copper chills for the development of Hematite particulated

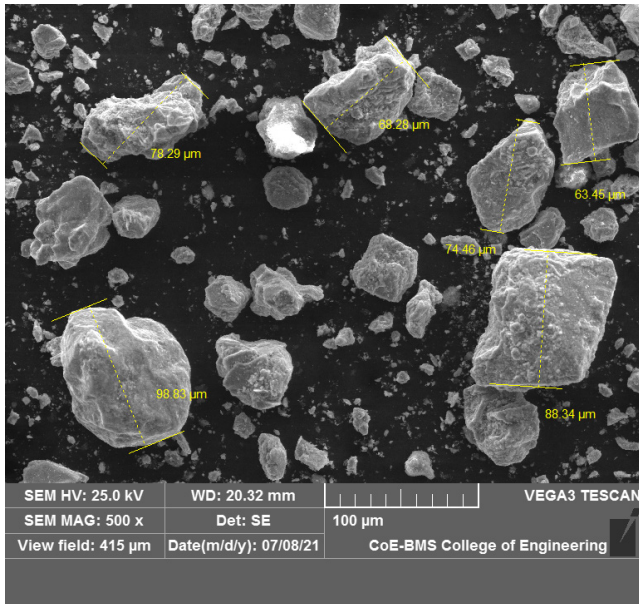


Figure 1. SEM images of Hematite particles of sizes 80-100 μm .

reinforced aluminium A356 composites using ducom-type fatigue testing equipment. EDAX, XRD, and SEM photos are studied for the presence of reinforcement and microstructure in the developed composites. The composites are casted with copper chills revealing superior fatigue strength as compared to the composites without copper chills.

2.0 Methodology and Experimental Investigations

2.1 Material Selection

In this research work, Alloys of A356 in ingot form was selected as a matrix material due to an extensive choice of applications in automobiles and aerospace industries. The particulated Hematite of size 80–100 μm was selected as reinforcement as shown in Figure 1. The chemical composition of both the reinforcement and matrix materials are given in Tables 1 and 2 respectively. The other properties of both materials are given in Tables 3 and 4 respectively.

2.2 Composite Preparation

The metal matrix composite of A356 alloys reinforced with particulate Hematite was developed by the stir casting method which is explained as follows. The A356

alloy being melted in (6kW) electric resistance oven up to 752°C with a 560 rpm stirring speed is maintained as exposed in Figure 2. The particulates of Hematite were warmed at 400°C and poured into the furnace consisting of a molten metal alloy of A356 (at 750°C). Continued the stirring for up to several minutes. Finally, constant stirring is ejected well wetting between the reinforcement and matrix. The prepared molten metal was dispensed into a preheated sand mould comprising with and without copper chills as shown in Figure 3. The casting process was repeated for different compositions of reinforcement with matrix material (weight proportions of Hematite Particles with base alloy from 0 wt% to 12 wt% in steps of 3 wt%). Casting was continued by preparing sand mould with copper chills as shown in Figure 4 for different compositions of reinforcement with a dimension of 170 \times 200 \times 25 mm^{22,23}.

2.3 Experimentation

A rotating-bending type low cycle fatigue test machine (made by Ducom Instruments, Bangalore), with model number TM7001 was used to conduct the fatigue tests at room temperature according to ASTM E606 standards along with specimen attachment as shown in Figure 6a and b. The specifications of the Ducom machine as shown in Table 5. The fatigue specimen having a diameter of 6.35 mm and length of 101.6 mm was machined in cast composite as shown in Figure 5¹⁰. During the tests, the cyclic frequency was 50 Hz (3000 revs/min constant) and the stress ratio (R) was -1. The fatigue life (Nf) of a sample is the number of cycles until complete separation or failure occurs. The gauge segment of the test samples was maintained at a constant surface finish of 1 μm by using increasingly finer grades of emery paper subsequently machining to minimize the effect of surface irregularities. In the tests, the maximum stresses varied from 50-200 MPa, which represents 50-90% of the yield strength of each material. The average of three results was used to find out the fatigue life (Nf) of each sample. The fatigue specimen before and after the test is shown in Figure 7¹³.

The equation can be considered by using stress-number of cycles of failure curve. Both without and with copper chill composites were conducted. The stress produced in test samples due to fatigue is calculated from the experimentation using the equations (For rotating bending type).

$$\text{Stress } \sigma_b = M_b / Z \quad (1)$$

Table 1. Chemical Composition of Alloy of A356

Composition	Percentage
Si	7.25
Mg	0.45
Fe	0.086
Cu	0.010
Mn	0.018
NI	0.025
Zn	0.005
Others	0.028
Al	92.12

Table 2. Chemical Composition of Hematite

Composition	Percentage
Fe ₂ O ₃	81.13
MnO	0.14
MgO	1.55
TiO ₂	0.03
Al ₂ O ₃	0.57
Cao	4.8
SiO ₂	4.2
Thrashing of detonation	7.58

Table 3. Properties of A356 Alloy

Properties	Units	Values
Density	gm/cc	2.67
Colour	----	Silver
Hardness (Brinell)	----	70–105
Tensile strength ultimate	Mpa or N/mm ²	234
Tensile strength yield	Mpa or N/mm ²	165
Compressive strength	Mpa	650
Elastic Modulus	Gpa	70–80
Poisson's Ratio	Nu	0.33
Melting Point	°C	557–613

Table 4. Properties of Hematite particles

Properties	Units	Values
Particle Size	Mm	80–100
Density	gm/cc	5.17
Colour	----	Red
Hardness (Mohr's Scale)	Kg/mm ²	5.5–6.5
Tensile strength	Mpa or N/mm ²	350
Elastic Modulus	Gpa	211
Poisson's Ratio	Nu	0.35



Figure 2. Electric Furnace.



Figure 3. (a) Mould with Copper chill, (b) Mould without Copper chill.



Figure 4. Prepared A356-Hematite composite with copper chills.

where M_b - Bending Moment,

$$\text{Bending Moment } M_b = FL/4 \quad (2)$$

Z- Section Modulus

$$\text{Sectional modulus } Z = \pi d^3/32 \quad (3)$$

The specimens of microstructure were developed for microscopic observation through a typical metallographic procedure, etched with Keller's reagent, and examined under the SEM Microscope. Figure 14 shows the microstructure with different weight fractions of copper chill samples. For analyzing the size, shape, and dispersion of Hematite particles existing in A356 alloy mixtures, an SEM device (TESCAN VEGA 3 LMU, Czech Republic) was used. For EDX investigation JDE 2300 software was used that linked with the SEM device. For microstructure 15 mm diameter and 5 mm, height specimens were examined in SEM. The surface of the specimen was ground (using 240, 600, and 800 grind paper) and polished with 44- μm thickness shining paper. It was operated on the polishing machine using velvet material to achieve a smooth surface finish. To remove impurities like dust or foreign particles present on the polished surface, the specimens were cleaned with distilled water. The surface of the samples was finally engraved by Keller's reagent¹⁷.

To recognize different phases in Al alloy matrix mixtures X-ray diffraction studies were conducted on A356 alloy composites. For XRD studies, A356 alloy with 9wt% of Hematite composites was chosen with specimen dimensions of 15mm diameter and 2mm height. XRD studies were conducted using PANALYTICAL XRD with Cu K α radiation, and the 2θ range is designated to cover all the intense peaks of the segments of material that are predictable¹⁸.

Fractography of the samples is taken to visualize the zones of fatigue, in which the stress is fully reversed; the uniform striations with the random locations of crack fronts can be seen in the fractography taken by SEM¹⁶.

3.0 Result and Discussion

3.1 Microstructure Investigation

The micrograph results show that particulates of Hematite appear to be discrete uniformly all over the A356 matrix at diverse weight fractions, as displayed in Figures 8(a-e). This can be attributed to the effective stirring achieved through the use of suitable process parameters. Using Homogeneous dispersion on elements of Hematite will enhance the fatigue strength of the mixtures and the rapid chilling rate will enforce fine-grained structure by using copper chill, which will also improve fatigue performance¹⁹.

Figure 9 displays the elemental scrutiny of A356 with 9 wt% of Hematite mixture which approves the existence of elements such as Al, Fe₂O₃, MgO, Cu, CaO, Zn and Si, The distribution of Hematite particles in A356

Table 5. Specifications of Ducom machine

Collet size	12mm
Normal Load	50–100 N
Speed	1000–5000 rpm
Speed accuracy	1 \pm 1% of measured speed
Bending moment	up to 500 Nm
Test duration	up to 999,999 cycles (max)
Machine dimensions	950 \times 500 \times 1140 mm
Controller dimensions	300 \times 290 \times 135 mm

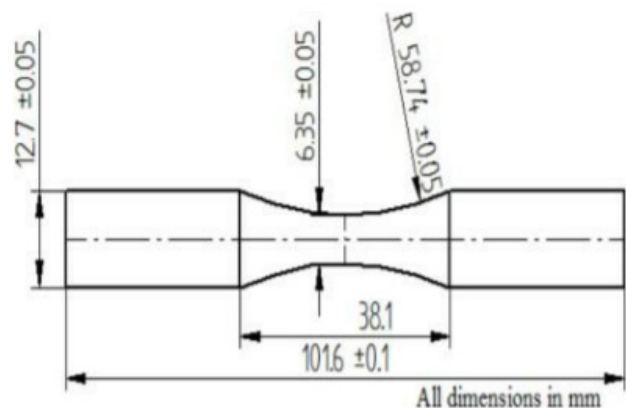


Figure 5. Standard specimen for fatigue test.



Figure 6. (a) Fatigue Testing machine, (b) Fatigue Testing machine with specimen attachment.

alloy mixture is confirmed by the existence of Fe_2O_3 and MgO . XRD analysis was carried out using an X-ray-diffractometer on the alloy of A356 and A356-9wt% of Hematite composites. Figure 10(a) represents A356 alloy XRD pattern with different phases of aluminium available at various peaks 39° , 45° , 65° , and 78° C with numerous intensities. 39° C is the uppermost intensity of the phase of Al. Further Figure 10 (b) shows the XRD pattern of A356

alloy with 9 wt% of Hematite particulates. It specifies the several phases like Fe_2O_3 and Al phases. The JCPDS form of the manufactured Al-Hematite fusions is 98-6077 with varied angles at 2θ with varying intensities, while particles of Hematite phases are identified at 29° , 47° , 56° and 78° C^{19,20}.

3.2 Fatigue Strength

Figures 11 and 12 show the outcome of stress vs. number of cycles for A356-Hematite particulate composites without and with copper chill conditions. From the experimental results, it was found that fatigue strength of A356-Hematite composites is larger than their un-reinforced alloy. The addition of Hematite particles in matrix alloy improved the fatigue life of the specimens. The fatigue strength of the composite improved with improvements in the content of Hematite elements both without and with copper chill circumstances. The development in the fatigue strength of the developing mixtures remains important at a lesser stress levels than the greater stress level in both without and with copper chill composites¹¹. In both cases the maximum heaviness proportion of Hematite elements showed substantial development in fatigue strength of the mixtures as associated with an unstrengthened alloy, this is due to the existence of solid Hematite elements. The consistent size and dispersal of Hematite elements over the composites enhance the plastic strain necessary for crack initiation into the composite materials. The fatigue strength increases with the volume segment of the elements due to the weight existence transmitted to the harder particulate strengthening and overall reduced strains for specified fatigue stress. The creation of voids leads to the proliferation of cracks at a quicker rate. Chilled specimens show higher fatigue strength than cast specimens. Because of poor wettability, fatigue strength increases up to 9% of reinforcement and decreases at 12% of reinforcement¹⁵.

3.3 Fractured Surface Analysis

Figure 13 (a-d) shows the fatigue fracture surfaces of A356-Hematite 9wt% composites with and without a copper chill. The following combinations of fracture modes are evidently present in fractured surfaces as discussed below:

- A crack initiates and propagates in a matrix substantial.
- Fracture and Decohesion of reinforced particles.

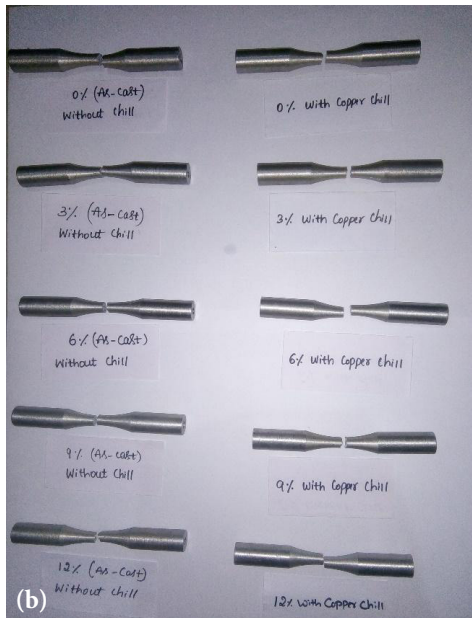
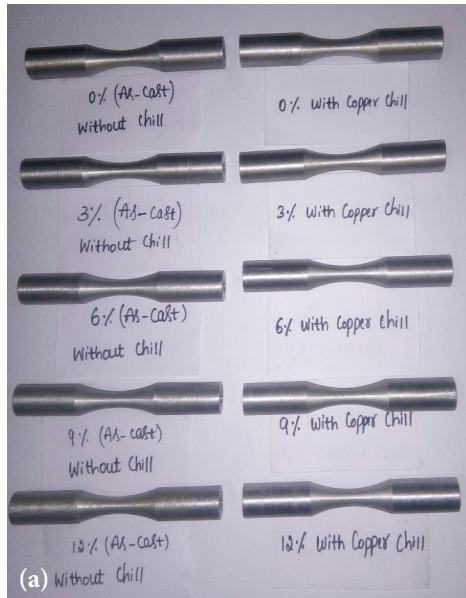


Figure 7. Fatigue Specimen (a) before and (b) after test.

- Development of macro and micro voids in the matrix substantial.
- Fractographic study.

The surface of a fractured area without copper chill composite consists of dimples, macro- and micro-voids (Figure 13 (a)). The chilled composite, on the other hand, has micro-voids and has limited ductility (Figure 13 (b)). Figure 13 (c) depicts the cracking initiation for a 9wt% composite without copper chill. It is evident from the SEM images of the fractured surface that, the

crack initiation in the 9wt% of the composite without copper chill is associated with the presence of porosity. The existence of porosity acts as a stress concentrator and facilitates crack initiation. Further, the crack is seen to have originated from the surface (Figure 13 (a)) without copper chill composite. There was no indication of particle decohesion or fracture can be seen in the region around the crack. In addition, particle fracture has been observed in several regions of chilled composites (Figure 14). Thus, it is evident that crack opening is due to surface imperfections/porosities in composites without copper chill and not at the matrix-particle interface region¹³.

Since the crack originated at the defective point, it propagated along the regions of a weakest portion (i.e. in the alloy of the matrix), due to the existence of reinforced elements that act as robust obstacle (Figure 15). When various microspities in the alloy of the matrix interrelate

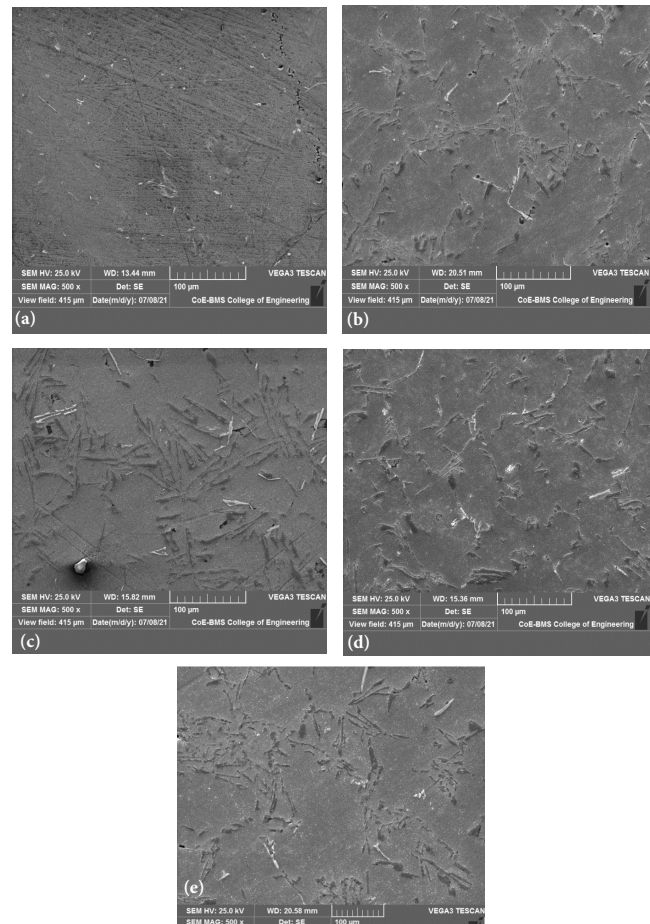


Figure 8. SEM Micro-graphs of (a) A356 alloy, (b) A356-3 Wt% of composite, (c) A356/6wt% composites, (d) A356/9wt% composite, (e) A356-12 Wt% of composite with copper chill at 500X magnification at chill casting conditions.

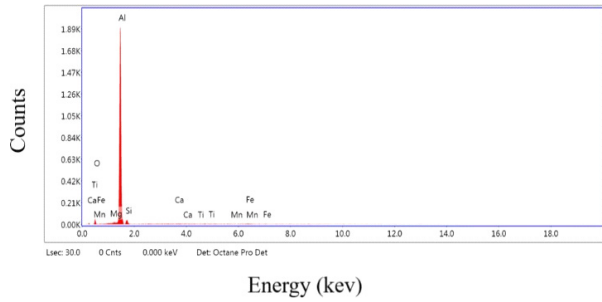


Figure 9. EDS spectrum of A356 with 9wt% of Hematite particulate composite showing the presence of Fe_2O_3 particles.

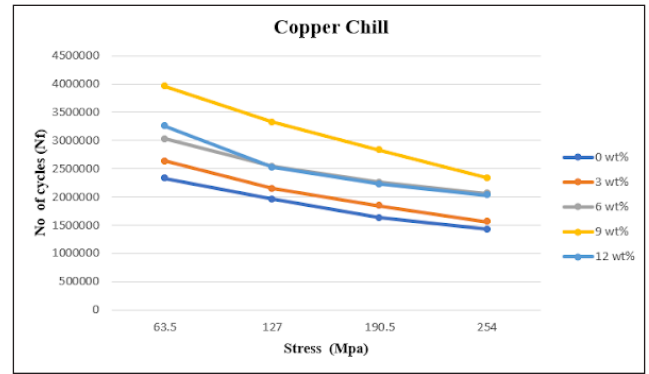


Figure 12. Stress vs. number of cycles for A356-Hematite particulate composites with copper chill condition.

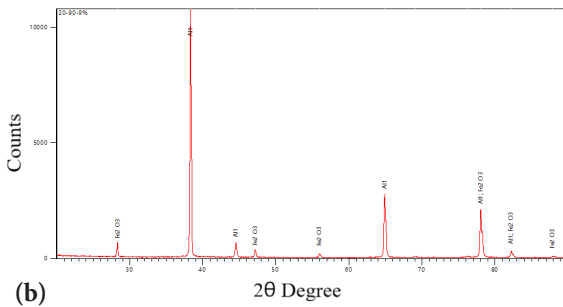
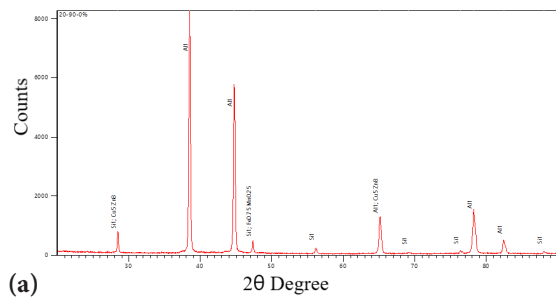


Figure 10. (a) X-ray diffraction of A356 alloy, (b) X-ray diffraction of A356-9wt% of hematite.

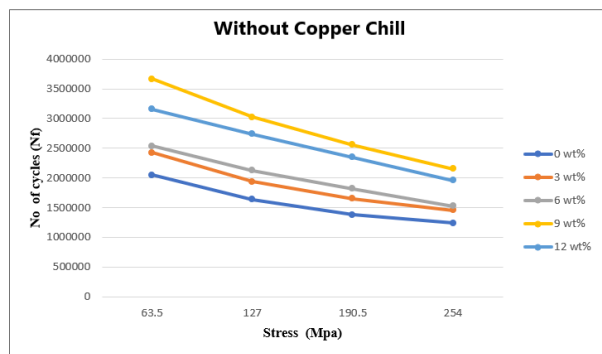


Figure 11. Stress vs. number of cycles for A356-hematite particulate composites for without copper chill condition.

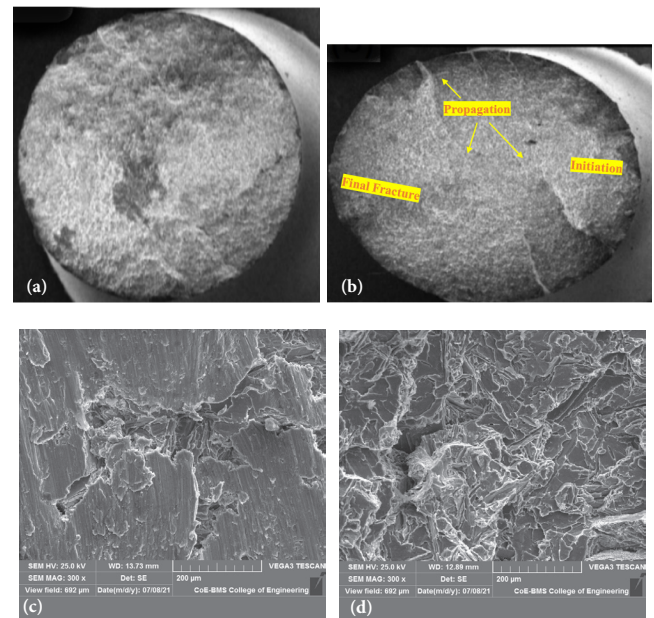


Figure 13. (a) A356-Hematite 9wt % of composite without copper chill, (b) A356-Hematite 9wt % of composite with copper chill, (c) Crack In A356-Hematite 9wt % of composite without copper chill, (d) crack In A356-Hematite 9wt % of composite with copper chill.

through the crack, causing the growing proportion of the crack is very high. The matrix region about the reinforced segment exhibits the micro-voids due to condensed ductility of matrix alloy¹⁵.

Though the crack propagation and initiation in the matrix region of chilled composites are away from the particles, so there is no cracks are observed at the interface (Figure 16).

It has been found that without copper chill mixtures have multiple crack initiation points (Figure 17). But, in chilled composites, crack initiation points are significantly

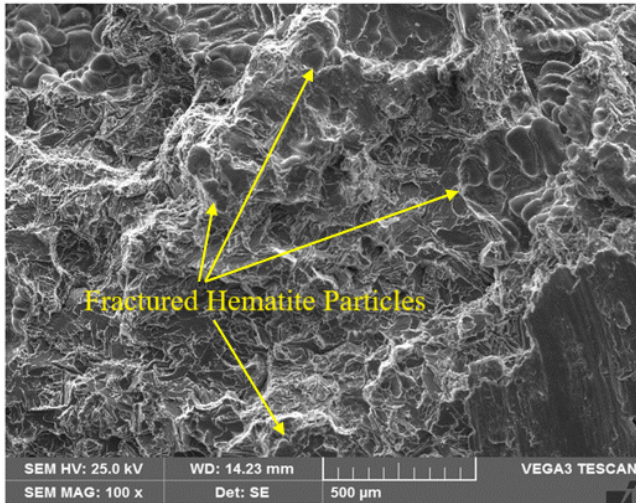


Figure 14. Fractured surface of cast A356-Hematite 9wt% of composite with copper chill shows fracture of armored particles.

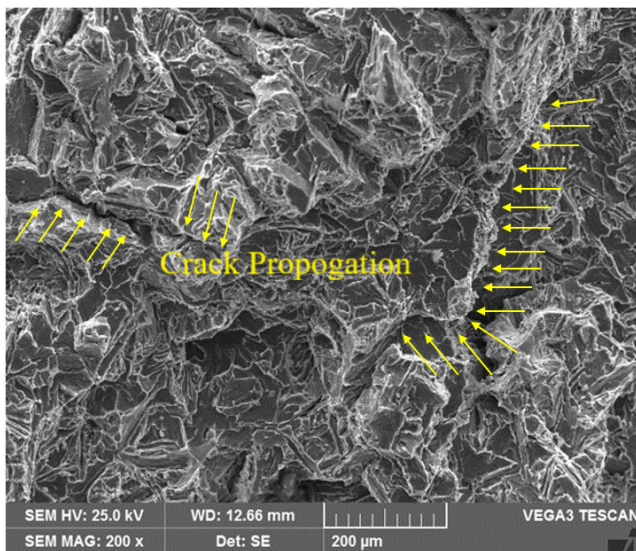


Figure 15. A356-Hematite composite displays the crack propagation regions.

fewer. Because of the huge volume fraction and unvarying spreading of Hematite particles, crack propagation is limited after crack initiation in composites. The crack proliferation velocity is constantly higher in composites without copper chill due to limited restraints. However, the propagation of cracks has remained restricted in the chilled composites due to the large constraints. Hence, the principal mechanisms of fracture in chilled composites are the creation of micro-voids in the matrix and cracks in the particles of reinforcement. The fracture

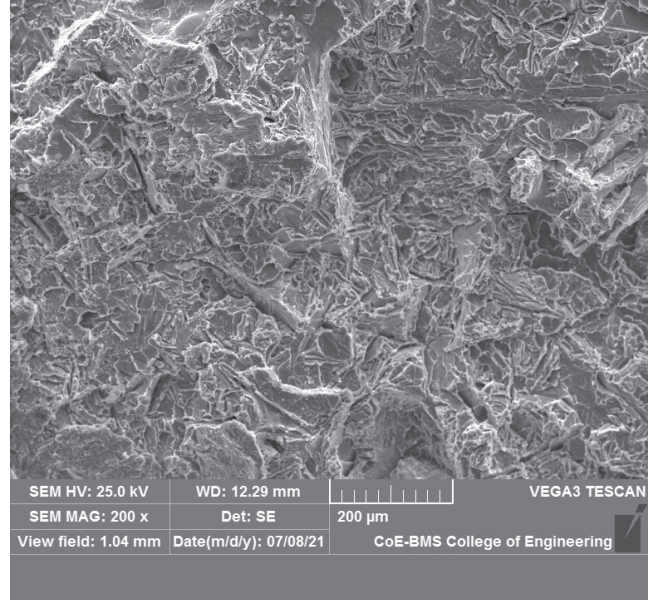


Figure 16. Fractured surface of chilled A 356-Hematite 9wt% of composite displays crack commencement and circulation in matrix region.

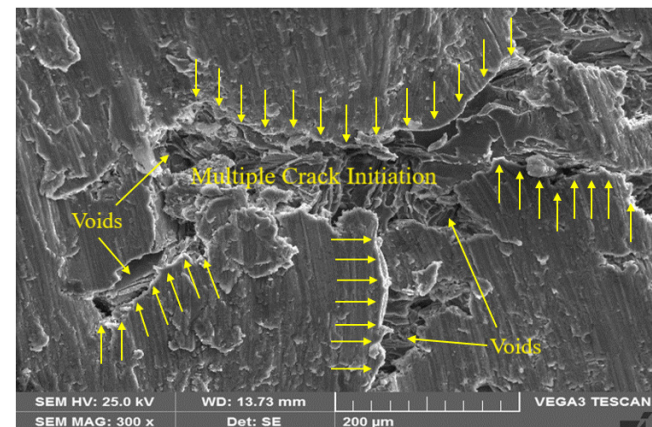


Figure 17. Multiple crack initiation in A356-Hematite 9wt % of composite without copper chill.

in the chilled composites has flat (flat fractured) surfaces due to the partial ductility of the matrix, indicating brittle fracture (Figure 18).

The chilled A356-Hematite composites exhibit large quantities of voids due to the brittle flow of matrix material and decohesion of reinforcement phases. It also seems that the bigger sized armored elements have remained fractured also decohesion has ensued with the minor sized elements. A few of the voids has been found in fractured surfaces have a diameter that is greater or smaller than the normal size of the reinforced elements^{11,13}.

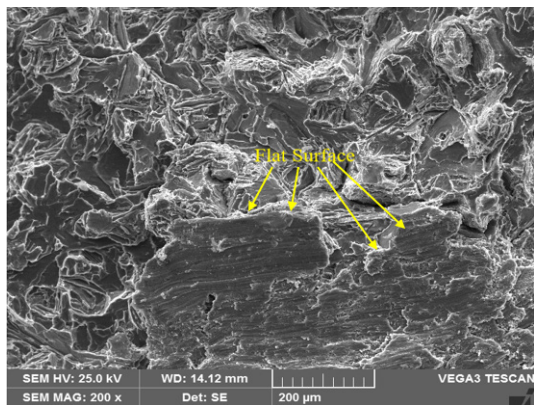


Figure 18. Fractured surface of chilled A356-Hematite 9wt% of composite shows a flat surface.

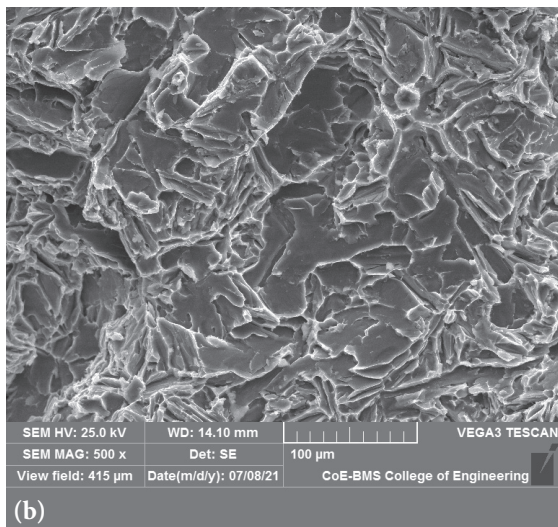
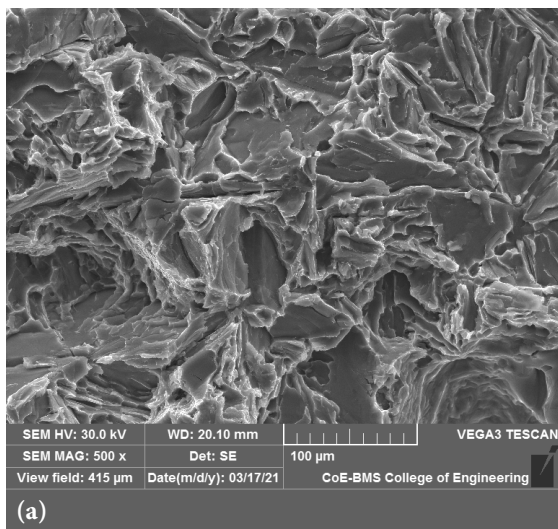


Figure 19. Fractography of A356/9wt% composite (a) with copper chill at 500X magnification, (b) without copper chill at 500X magnification.

3.4 Fractography

Figure 19 (a) (b), shows that clear inferences are often drawn by reference to the method of fracture which is a brittle one, shown by the cleavage facets from the transgranular crystallographic plane and cleavage is a representative of transgranular brittle fracture¹⁹. An intergranular fracture can be identified by the appearance of a “rock candy structure” when the crack follows grain boundaries. The semi-elliptical lines observed in the fractograph are a sign of striations. That arises outward from the origin and marks the crack front location with each successive stress cycle. The arrangement of fatigue striations is typically uniform. The crescent-shaped marks can be referred to as “beach marks” and indicates the succeeding stages of advanced crack growth that ensure due to variations in loading or varying stress intensity. In order to analyze the failure mechanism within a component, the fractograph of a fatigue specimen is precious¹⁷.

4.0 Conclusions

A356-Hematite particulate reinforced amalgams were developed through sand casting practice without and with a copper chill. The following conclusions were made:

- The Microstructural study evidently displays the uniform spreading of Hematite elements in the matrix of A356 alloy and its mixtures.
- The XRD examination affirms the presence of Hematite particles and their phases in the A356 alloy matrix.
- The number of cycles to failure and fatigue strength of A356-Hematite composites was predicted using a Rotating Bending Machine (RBM-ASTM E606 standard). It was found that the composite having a composition of 9wt% Hematite reinforced with A356 alloy is exhibits strong fatigue strength as associated with other compositions and it is also found that the specimens of copper chilled composite is stronger than those without copper chill composites due to the existence of iron oxide and the magnesium oxide in the composites which also influences in an increase of fatigue strength by enhancing hardness and toughness.
- Both without and with copper chill composites, there was an improvement in fatigue strength at lower stress levels (63.5 MPa) compared to higher stress levels (254 MPa).

- The composite cast with copper chill shows higher fatigue strength as compared to the composite cast without copper chill due to the presence of hard ceramic elements of Hematite (iron oxide and magnesium oxide).
- From the fractured surface analysis and fractography, it clearly shows the crack commencement is due to the surface defects/porosities in the alloy of matrix and not in the area of matrix and particle interface. And also the method of fracture is brittle in nature, signified by the cleavage facets from the transgranular crystallographic plane and striations.
- From the overall results, it is concluded that the Hematite act as a major role in enhancing the fatigue behaviour of aluminium matrix composite.

5.0 References

1. American Society for Metals, ASM Handbook, Properties and selection. Nonferrous Alloys and Special-purpose Materials, ASM International hand book committee. 1990; 2:137-38.
2. MEIM. Schwartz, Composite material hand book, McGraw Hill, Newyork. 1984.
3. Heinz A and Haszler A. Recent developments in aluminium alloys for aerospace applications, Material Science and Engineering. 2000; 1:102-107. [https://doi.org/10.1016/S0921-5093\(99\)00674-7](https://doi.org/10.1016/S0921-5093(99)00674-7)
4. KHW Seah, J Hemanth, SC Sharma and KVS Rao. "Solidification behavior of Water-Cooled and subzero chilled cast iron" Journal of alloys and Compounds. 1999; 290:172-180. [https://doi.org/10.1016/S0925-8388\(99\)00224-8](https://doi.org/10.1016/S0925-8388(99)00224-8)
5. Haider Tawfiq Naem, Firas Fouad Abdullah. "Effects of garnet particles and chill casting conditions on properties of aluminum matrix hybrid composites". Ecletica uimica Journal. 2019; 44(2):45-52. ISSN: pp. 1678-4618. <https://doi.org/10.26850/1678-4618eqj.v44.2.2019.p45-52>
6. Anupama Hiremath, Joel Hemanth. "Experimental Evaluation of the Chill Casting Method for the Fabrication of LM-25 Aluminum Alloy-Borosilicate Glass (p) Composites". Advanced Materials and Engineering Materials. VI ISSN: 1662-9795. 2017; 748:69-73. © Trans Tech Publications, Switzerland. <https://doi.org/10.4028/www.scientific.net/KEM.748.69>
7. Vasanth Kumar HS, UN Kempaiah, G Malleesh. "Fatigue and Fracture Behaviour of Al6061-B4C Aluminium Matrix Composites". International Journal of Engineering and Advanced Technology (IJEAT). 2020; 9(4):2121-2125. <https://doi.org/10.35940/ijeat.D9166.049420>
8. Mahendra HM, GS Prakash, Keerthi Prasad KS, Rajanna S. "Fatigue and Fracture Behaviour of Al6061-Al2O3 Metal Matrix Composite: Effect of Heat Treatment". IOP Conf. Series: Materials Science and Engineering. 2020; 925:012042. ICCEMS-2020. <https://doi.org/10.1088/1757-899X/925/1/012042>
9. Krishnaraj S, Elatharasan. "Fatigue behaviour of aluminium reinforced metal matrix hybrid composites" International journal of rapid manufacturing. 2020; 9(1). <https://doi.org/10.1504/IJRAPIDM.2020.104417>
10. Sanju H, Meghani Moulis Reddy, Batluri Tilak Chandra, Madhu B. "Evolution of Fatigue and corrosion test of Al LM13 reinforced with Hematite". International journal of research in Engineering and Technology. 2016; 5(6):219-223. <https://doi.org/10.15623/ijret.2016.0506040>
11. Achutha MV, Sridhara BK, Abdul Budan. "Fatigue Life Estimation of Hybrid Aluminium Matrix Composites". International Journal on Design and Manufacturing Technologies. 2008; 2(1):14-21. <https://doi.org/10.18000/ijodam.70022>
12. DP Myriounis, TE Matikas, ST Hasan. "Fatigue Behaviour of SiC Particulate-Reinforced A359 Aluminium Matrix Composites". An International Journal for Experimental Mechanics. 2012; 48:333-341. <https://doi.org/10.1111/j.1475-1305.2011.00827>
13. S Ramesh, N Govindaraju, CP Suryanarayan. "Investigation on Mechanical and Fatigue behaviour of Aluminium Based SiC/ZrO2 Particle Reinforced MMC". IOP Conf. Ser.: Mater. Sci. Eng. 2018; 346:1-8. <https://doi.org/10.1088/1757-899X/346/1/012030>
14. Girija Moona, RS Walia, Rastogi Vikas, Rina Sharma. "Parametric optimization of fatigue behaviour of hybrid aluminium metal matrix composites". Materials today proceedings. 2019; 21. <https://doi.org/10.1016/j.matpr.2019.10.002>
15. CS Ramesh, R Keshavamurthy, J Madhusudhan. "Fatigue behavior of Ni-P coated Si3N4 reinforced Al6061 composites". ICMPC 2014, Procedia Materials Science. 2014; 6:1444-1454. <https://doi.org/10.1016/j.mspro.2014.07.124>
16. Srivatsan TS, Meslet Al-Hajri, Petraroli M, Hotton B, and Lam PC. "Influence of Silicon carbide particulate reinforcement on quasi static and cyclic fatigue fracture behavior of 6061 aluminium alloy composites". Journal of Material Science and Engineering. Elsevier. 2002; 325:202-214. [https://doi.org/10.1016/S0921-5093\(01\)01444-7](https://doi.org/10.1016/S0921-5093(01)01444-7)
17. Umesh H, Suresh N, Sundresh S. "Fatigue Behaviour of Fly ash Reinforced with LM6 Aluminium Metal Matrix Composite". International Journal of Advances In Scientific Research and Engineering. (IJASRE). 2016; 2(9):1-13.
18. Ceschini L, Minak G, Morri A. "Tensile and fatigue properties of the AA6061/20 vol.% Al₂O₃p and AA7005/10 vol.%

- Al₂O₃p composites”. *Composites Science and Technology*. 2006; 66:333–342. <https://doi.org/10.1016/j.compscitech.2005.04.044>
19. Santhosh N, Kempaiah UN, Ganesh Sajjan, Ashwin C Gowda. “Fatigue Behaviour of Silicon Carbide and Fly Ash Dispersion Strengthened High Performance Hybrid Al 5083 Metal Matrix Composites”. *Journal of Minerals and Materials Characterization and Engineering*. 2017; 5:274-287. <https://doi.org/10.4236/jmmce.2017.55023>
 20. Madeva Nagaral, RG Deshapande, V Auradi, Satish Babu Boppana, MR Anil Kumar. “Mechanical and wear characterization of ceramic boron carbide-reinforced Al2024 alloy metal composites”. *Journal of bio and tribo corrosion*. 2021:7-19. Springer. <https://doi.org/10.1007/s40735-020-00454-8>
 21. Sunil Kumar M, Sathisha N, Jaganatha N, Batluri Tilak Chandra. “Tribological study on effect of chill casting on aluminium A356 reinforced with Hematite paticulated composites”. *Journal of Bio and Tribo Corrosion*. 2022; 8(52). Springer. <https://doi.org/10.1007/s40735-022-00635-7>
 22. Nagaral M, Auradi V, SA Kori, Hiremath V. “Investigation on mechanical and wear behavior of nano Al₂O₃ particulates reinforced AA7475 alloy composites”. *Journal of Mechanical Engineering Science*. 2019; 13:4623-4635. <https://doi.org/10.15282/jmes.13.1.2019.19.0389>
 23. Sunil Kumar M, Sathisha N, Batluri Tilak Chandra. A study on effect of chill casting on A356 reinforced with Hematite metal matrix composite, *Materials Today Proceedings*. 2021; 35(3):450-455. <https://doi.org/10.1016/j.matpr.2020.02.963>